



## Investigating the Effect of Considering Different Cross Section Design in Friction Stir Welded Joint Line of Dissimilar Aluminum Alloys

M. Tamjidi<sup>\*a</sup>, K. Danesh Narooei<sup>b</sup>

<sup>a</sup> Department of Industrial Engineering, Velayat University, Iranshahr, Iran

<sup>b</sup> Department of Industrial Engineering, Faculty of Industry and Mine Khosh, University of Sistan and Baluchestan, Zahedan, Iran

### PAPER INFO

#### Paper history:

Received 28 June 2022

Received in revised form 13 September 2022

Accepted 18 September 2022

#### Keywords:

Friction Stir Welding  
Cross Section in Joint Line  
Tensile Properties

### ABSTRACT

Using friction heat, welded joints of the Friction stir welding (FSW) process are made that are utilized to forge metal components together. Since there is no parent metal melting, several advantages are obtained by the FSW process over fusion welding. The alloys AA6XXX and AA7XXX Al are two sets of the most extensively utilized structural materials in rail transportation, automotive, and aerospace industries. The objective of present study was to investigate the effects of novel cross-sections in joint lines and further analyze the improvement in mechanical features. Due to the importance of the weld zone properties, many researchers seek to improve the mechanical behavior of the weld zone. For this, friction stir welded joint under four different new design in cross section named E1, E2, E3, E4 and one conventional cross section, E5 were conducted. Better outcomes are obtained by joints made utilizing this method based on joint quality and strength. The very good tensile features are displayed by the fabricated joints with Ultimate Tensile Strength (UTS) > 254 MPa and elongation > 7%. The highest UTS value which is occurred in E3 condition (Downward step) is 24.7% higher than required for FSW of AA6061 alloy at T6 condition in the American Welding Society (AWS) standard (186 MPa).

doi: 10.5829/ije.2023.36.01a.03

## 1. INTRODUCTION

The Welding Institute (TWI) developed friction stir welding (FSW) in 1991, which is employed successfully to weld aluminum alloys, mainly 2XXX or 7XXX series aluminum alloys. Welding these alloys is difficult through conventional thermal welding approaches [1, 2].

FSW is an emergent solid-state joining procedure where the welding material is not melted and recast, rather it can be arranged as the butt weld (Figure 1). The lower cost reduced weight by joining light-weight metals with metallurgical features, and a reduced requirement for skilled people make FSW an attractive welding technique [3]. Moreover, the higher energy efficiency and eco-friendliness make FSW a "green" procedure [4]. Utilizing this welding technique, it becomes possible to decrease energy consumption by 99% and installation cost by 40% compared to resistance spot welding [5].

Moreover, FSW is a hot-shear solid-state joining process using a non-consumable rotational instrument for producing frictional heat at the welding location with no material melting. It forms a smaller temperature gradient and defect-free joints than the conventional arc procedure [6].

The cost and quality of the completed weld can be affected by the joint design. Determining the most suitable joint design for a welding need special attention. Each of weld joint designs for a job requires to be compromised. For instance, this compromise can be between strength and cost, equipment available and welded skill, or between any two, three or more factors. Thus, an appropriate joint design requires experience. Even having experience, trial welds are necessary before selecting the final joint configuration and welding parameters [7]. The term weld joint design can be defined as the way that two pieces of metal are put together or

\*Corresponding Author Institutional Email: [m.tamjidi@velayat.ac.ir](mailto:m.tamjidi@velayat.ac.ir)  
(M. Tamjidi)

aligned with each other. The five basic weld joint designs are butt joints, lap joints, tee joints, outside corner joints, and edge joints [8].

The joint has reasonably higher strength. However, its use is not proposed when the metals are under impact loads or fatigue. This joint is simply prepared since it only requires matching the plates' edges together [6]. Though, correct fitting is important for the joint's total length as with any other joint.

In soldering, braze welding, and brazing, the finished part's tensile strength is highly affected by the space between the joining parts greatly. By heating the parts, the initial space may decrease or increase, based on the joint fixturing and design. Increasing the area being joined can increment the strength of a butt joint. The parts with the thickness of 1/4 in. (6 mm) need to be not considered for soldering or brazing when another process will successfully work. There are three basic joint designs in brazing including lap, butt and scarf (Figure 1). It is worth noting that a scarf joint is a type of butt joint where an increased area of bond is presented without incrementing the bond's thickness [9]. The area of a bond is based on the scarf angle cut for the joint.

In addition to the above-mentioned joint design, there is a method known as splice joint where two members are joined end to end in woodworking. The splice joint is utilized when no required length of the material being joined exists. It is a substitution for other joints like the scarf joint and butt joint. Splice joints are more robust than unenforced butt joints. They are potentially stronger than a scarf joint [10]. Three main kinds of splice joints were considered including bevel lap, half lap, and tabled splice joint (Figure 2). The half-lap splice is the most prevalent type of the splice joint.

As previously stated, the FSW process is solid state welding process in which an inconsumable rotation pin is inserted into the adjoining edges of the metals to be welded with a proper tilt angle and then moved all along the joint. The pin generates frictional and plastic deformation heating in the welding zone [11]. Thus, tool movement parameters and tool geometry which can be controlled by operators are among the key factors that

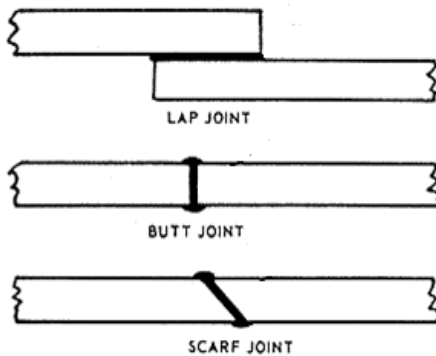


Figure 1. Three types of common joint designs for brazing

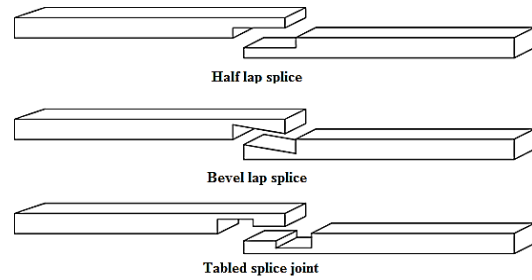


Figure 2. Three main types of splice joints

affect the quality of the fabricated joint and welding properties [12]. The terminology as described in Figure 3 is based on the international standard for FSW of aluminum (ISO 25239) [13]. Parameters which apply to FSW and are not mentioned in this standard, are previously explained in other standards such as the international standard for friction welding (ISO 15620) [14]. Other factors like work-piece thickness, material placement, machine characteristics and control mechanisms will also affect the weld quality [15].

Mechanical properties of FSW are paramount to industry, and is a very attractive field. The main particular areas of focus have been on tensile strength, yield strength, hardness/microhardness and percentage of elongation. Hardness tests can be used to not only ascertain an approximate strength of a material, but also see how strength varies from one part of a FSW to another. In butt welds tensile tests can be performed horizontally and vertically, where the nugget is either tested in the traverse direction or the longitudinal direction. Many studies relating to the dissimilar welding of aluminum alloys have been performed and reported in the literature. Table 1 classifies the previous works based on the mechanical properties of dissimilar FSW Al alloys. Also Table 2 lists the tool geometries, tool materials and welding variables used for FSW of dissimilar Al alloys in the literature.

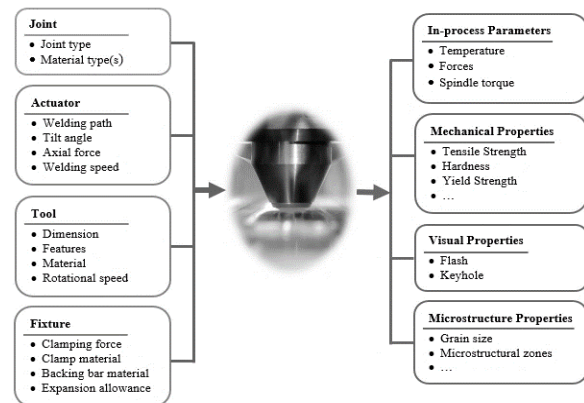


Figure 3. Input parameter influence FSW process (left) and the resulting output parameters (right) and welding properties

**TABLE 1.** Classification of pervious work on mechanical properties of dissimilar FSW Al alloys

Reference	Mechanical Properties		
	UTS	H	E
Azeez, et al. [16]	×	×	
Avinash et al. [17]	×	×	
Cole et al. [12]	×		
Haribalaji et al. [18]	×		
Prasanth and Raj [19]	×		×
Guo et al. [20]	×	×	
Kasman and Yenier [3]	×	×	
Kesharwani et al. [21]	×		×
Peng, et al. [22]	×	×	
RajKumar et al. [23]	×	×	
Heidarzadeh et al. [24]	×	×	×
Azeez et al. [25]	×		×
Venkateswarlu et al. [26]	×		×

This research is challenging since it needs to take into account the effects of various cross-sections in joint line (joint line design) for improving the mechanical features in dissimilar FSW of AA7075-T6 and AA6061-T6 aluminum alloys joints. This innovative technique can assist to present practical solutions to applications with difficulties in welding dissimilar alloys. Such applications are prone to the creation of harmful intermetallic compounds.

Therefore, the aim of this study is to investigate the effects of novel cross-sections in joint lines. Friction stir welded joint, In two different joint designs, called scarf joint and half lap splice joint, under four different new design in cross section named E1, E2, E3, E4 and one conventional cross section, E5 were conducted. Ultimate tensile strength (UTS), yield strength (YS), elongation (E) and minimum hardness (HV) of dissimilar FSW of AA6061-T6 and AA7075-T6 joints under process parameters found in the previous studies which are tool rotational speed of 1040 rpm, tool traversing speed 135 mm/min and tilt angle 2°. Rest of this paper is organized as follows: section 2 describes the experimental details,

**TABLE 2.** Literature review on tool material, profiles and welding parameters used for dissimilar Al alloys FSW

Reference	Workpiece material	Tool material	Tool shape and size	Operating parameters
Ahmad M. Z. et al. [27]	AA2024-T4 / (4 mm Thickness) AA7075-T6, (5 mm thickness)	H13	SD: 20 mm; PS: Threaded cylindrical; PD: 3.8 mm	RS: 400,600,800 rpm TS: 50 mm min <sup>-1</sup>
Avinash et al. [17]	AA2024, (5 mm) / AA7075, (6 mm)	H13	SD: 25 mm; PS: Square; PD: 5 mm; PL: 4.8 mm	RS: 710, 1000, 1400 rpm; TS: 80, 120 mm min <sup>-1</sup> TO: 1 mm towards AA2024
Cole et al. [12]	AA6061-T6 / AA7075-T6, (4.76 mm)	H13	SD: 15 mm; PS: Threaded conical; PD: 7 to 5.2 mm; PL: 4.7 mm	RS: 700-1450 rpm TS: 100 mm min <sup>-1</sup> MP: 6061-7075, 7075-6061 TO: -2 to 2 mm
Torzewski et al. [28]	AA7020-T651 / AA5038-H111, (5mm)	HSS	SD: 15 mm; PS: Cylindrical; PD: 5 mm; PL: 2.6 mm	RS: 400, 800, 1200 rpm TS: 100,200,300 mm min <sup>-1</sup> AF: 17 kN, TA: 2° RS: 1200 rpm
Guo et al. [20]	AA6061-T6 / AA7075-T6, (6.3 mm)	-	SD: 15 mm; PS: Threaded conical; PD: 5 mm	TS: 120,180, 300 mm min <sup>-1</sup> AF: 6-7 kN, TA: 2.5° MP: 6061-7075, 7075-6061
Kasman and Yenier [3]	AA5754-H111 / AA7075-T651, (5 mm)	H13	SD: 18-20-22 mm; PS: Threaded cylindrical ; PD: 6 mm; PL: 4.8 mm	RS: 1000-1200 rpm TS: 80-125 mm min <sup>-1</sup> TA: 3°, DT: 30 s
Kesharwani et al. [21]	AA5052-H32 / AA5754-H22, (2 mm)	SS-316	SD: 12-15-20 mm; PS: Circular, triangular, square; PD: 1/3 SD for circular pin; PL: 1.8 mm	RS: 1120, 1400, 1800 rpm TS: 50, 125, 200 mm min <sup>-1</sup>
Koilraj et al. [29]	AA2219-T87 / AA5038-H321, (6 mm)	H13	SD: 1.5- 3 (D/d ratio); PS: Straight and tapered cylindrical, cylindrical and tapered threaded; PD: 6 mm; PL: 5.7 mm	RS: 400-800 rpm TS: 15-60 mm min <sup>-1</sup>
RajKumar et al. [23]	AA5052 / AA6061	H13	SD:18 mm; PS: Threaded cylindrical ; PD: 6 mm; PL: 4.8 mm	RS: 710 rpm TS: 20, 28 mm min <sup>-1</sup>

Shojaeefard et al. [30]	AA7075-O / AA5083-O, (6 mm)	-	SD:20 mm; PS: Tapered ; PD: 10 mm to 5 mm; PL: 5.85 mm	RS: 500-1600 rpm TS: 30-90 mm min <sup>-1</sup>
Kumar et al. [31]	AA5083 / AA6061	HSS	PS: Tapered cylindrical, Tapered square, Tapered Hexagon, Paddle shape, Straight cylinder	RS: 800-1600 rpm TS: 40-80 mm min <sup>-1</sup> AF: 15-35 kN
Venkateswarlu et al. [26]	AA2219/ AA7039, (6 mm)		SD: 19 mm; PS: Threaded with three different shoulder surface PD: 7 mm; PL: 4.7 mm	RS: 500-1000 rpm TS: 20-40 mm min <sup>-1</sup> AF: 5-8 kN

SD: Shoulder Diameter; PS: Pin Shape; PD: Pin Diameter; PL: Pin Length; RS: Rotational Speed; TS: Traverse Speed; TO: Tool Offset; MP: Material Placement; DT: Dwell Time; TA: Tilt Angle; AF: Axial Force

section 3 presents the weld joint cross section design, section 4 results and discussion, and section 5 provides the final conclusion.

## 2. EXPERIMENTAL WORKS

Dissimilar aluminum alloys were chosen in this study such as AA7075 and AA6061 in the T6 temper circumstances for butt scarf welding by FSW procedure. Both plates with a thickness of 6 mm were cut before welding to a length of 100 mm and a width of 50 mm. The FSW weld direction is vertical to the plates' rolling direction. Before implementing the experiments, the mechanical features of base aluminum alloys, AA6061 and AA7075 were measured. AA6061 and AA7075 have the ultimate tensile strength of 310.MPa and 524.MPa, and the elongation of the 12% and 11 %, respectively.

The experiments were performed using an instrument made of AISI H13 hot work steel with a square pin profile. To increment its wear resistance, it used to be heat-treated to a hardness of 52 HRC after machining (see Figure 4).

The ASTM E8M guidelines were followed in order to preparing the specimens for obtaining the real mechanical properties and fracture location of FSW welded joints for the sub size specimen. At slightest three examples were extracted from each FSWed joint following GOST ISO 25239-4-2020. The arrangement and measurement of each transverse tensile example device balanced position as shown in Figure 5.

## 3. WELD JOINT CROSS SECTION DESIGN

After validation of results conducted on the FSW butt joint configuration, the final step in this study is to consider the effect of different weld joint designs on the mechanical properties in order to improve the joint efficiency. In this study two joint designs, called scarf joint and half lap splice joint, were investigated from mechanical point of view using the experimental parameters found in the previous studies which are tool

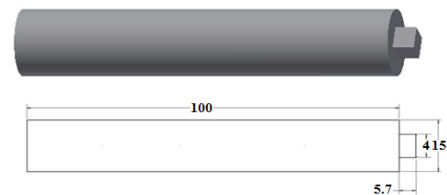


Figure 4. Geometry of tool design

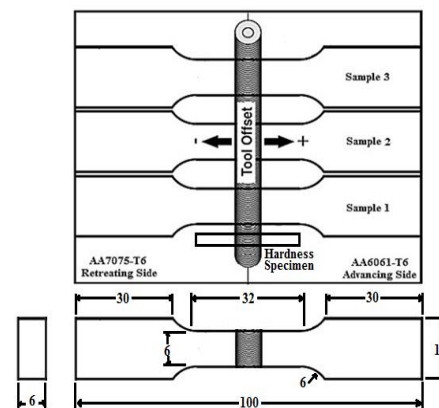


Figure 5. Arrangement and measurement of each tensile example device balanced position

rotational speed of 1040rpm, tool traversing speed 135 mm/min and tilt angle 2°. Figure 6 and Figure 7 illustrate the scarf and half lap splice joint design, respectively.

Figure 6(a) demonstrates a downward scarf joint cross section which represents the inclination from advancing side to retreating side and Figure 6(b) shows the upward scarf joint cross section in which the slope is expanded up from advancing side to retreating side.

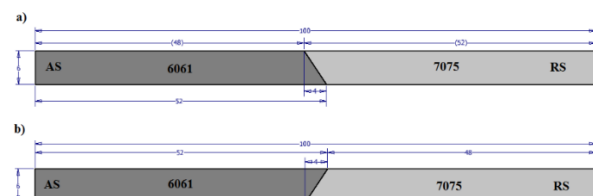


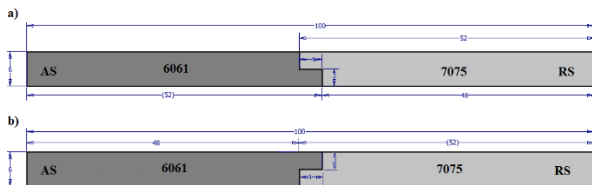
Figure 6. Interface design in weld line: a) downward scarf and b) upward scarf

Figure 7(a) demonstrates a downward half lap splice cross section design which represents the downward step from advancing side to retreating side and Figure 7(b) shows the upward step half lap splice cross section in which the step is expanded up from advancing side to retreating side.

In order to investigate the effect of different welding joint design on mechanical properties of the FSW joints, five experiments were performed using the optimal level of process parameters found in previous section. The detailed experimental conditions with their cross section are listed in Table 3. Dissimilar FSW joints were produced along the longitudinal direction of five plates of AA6061 and five plates of AA7075 were cut into measurements measuring 100 mm long and 52 mm wide (rolling direction) employing a Jonford milling machine as shown in Figure 8. The tensile testing of the FSW joints is conducted in exact Universal Testing Machine Instron 3382 and their ultimate tensile strength (UTS), YS, E are measured. A maximum of 31 measurements were taken on each sample spaced every 1 mm in the weld region and every 8 mm outside of the tools footprint. The microhardness plots will also highlight the differing weld regions.

#### 4. RESULTS AND DISCUSSION

Table 4 shows the mechanical properties of the base AA6061 and the various cross-sectional structural



**Figure 7.** Interface design in weld line: a) downward half lap splice and b) upward half lap splice

**TABLE 3.** Experimental conditions and cross section design

Condition	Weld cross section	Cross section appearance
E1	Downward scarf	AS 6061 / 7075 RS
E2	Upward scarf	AS 6061 / 7075 RS
E3	Downward half lap splice	AS 6061 / 7075 RS
E4	Upward half lap splice	AS 6061 / 7075 RS
E5	Butt joint	AS 6061 / 7075 RS



**Figure 8.** The Johnford vertical milling machine

connections between the AA6061 and AA7075. The mechanical properties of AA6061 are listed in this table. This is because all joints on the AA6061 side were damaged at the location of the HAZ region where the minimum hardness is shown in Figure 9. As detailed already in different FSW of other Al alloys, the friction stir welded joints ordinarily fractured at areas in HAZ on the weaker fabric side [15,25]. Furthermore it may, those researchers did not consider the impact of cross-section design on the mechanical properties. The disappointment areas in HAZ shows consistent holding has been accomplished between disparate AA6061 and AA7075 alloys beneath all examined welding conditions. According to Table 4, very exact tensile residences are represented by all the joints with UTS > 254 MPa and elongation > 7%. The maximum UTS value occurring in the E3 condition (Downward step) is 24.7% larger than the value needed for the FSW of AA6061 alloy at the T6 condition in the American Welding Society (AWS) standard (186 MPa): AWS D17.3/ D17.3M:200X.

The Vicker's microhardness profiles of the cross-section for the dissimilar joints made under various conditions (E1–E5) are shown in Figure 8. Generally, both AA7075 and AA6061 alloys represented definite microhardness reduction in the weld in comparison with their equivalent base metals (the two materials in T6 temper conditions).

The main reason is the dissolution, coarsening, and precipitation of strengthening precipitates resulting from FSW thermal cycles. However, there are some minor contributions associated with grain structure refinement. In the HAZ, coarsening of strengthening precipitates and the disappearance of Guinier–Preston (G.P.) zones cause a slightly lower hardness the same as an over-aging procedure. Further severe coarsening and probably complete dissolution of precipitates happened in the TMAZ, owing to the similar effects of treating the solution. In the nugget, some precipitation may occur after complete dissolution owing to the higher temperature for the material in this area. The transition of

microhardness is more gradual in the nugget from AA6061 to AA7075.

In all the cases (the marked arrows in Figure 8), irrespective of the applied process parameters or the relative materials' position, the hardness minima are observed in the HAZ on the AA6061 side. Indeed, in HAZ regions, all joints had a failure on the AA6061 side near the TMAZ in tensile testing, in which the minimum hardness is placed. The reduced microhardness in HAZ is caused by the disappearance of G.P. zones and coarsening of the strengthening precipitates which it can be seen in Figure 9. Therefore, in the HAZ of the joints made with less heat input, less severe precipitate coarsening could happen. Thus, the highest minimum value is obtained by the hardness profile of the joints made with the least heat input (condition E3) (Figure 8).

Figure 10 represents the tensile tested samples' fractured surfaces under SEM for circumstances E3 and E5. Fractographic analysis was performed using these two circumstances since UTS is the key objective

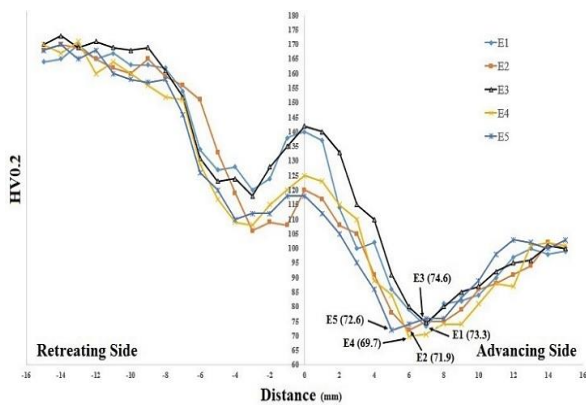


**Figure 9.** Vicker's microhardness profile of different cross-section joints

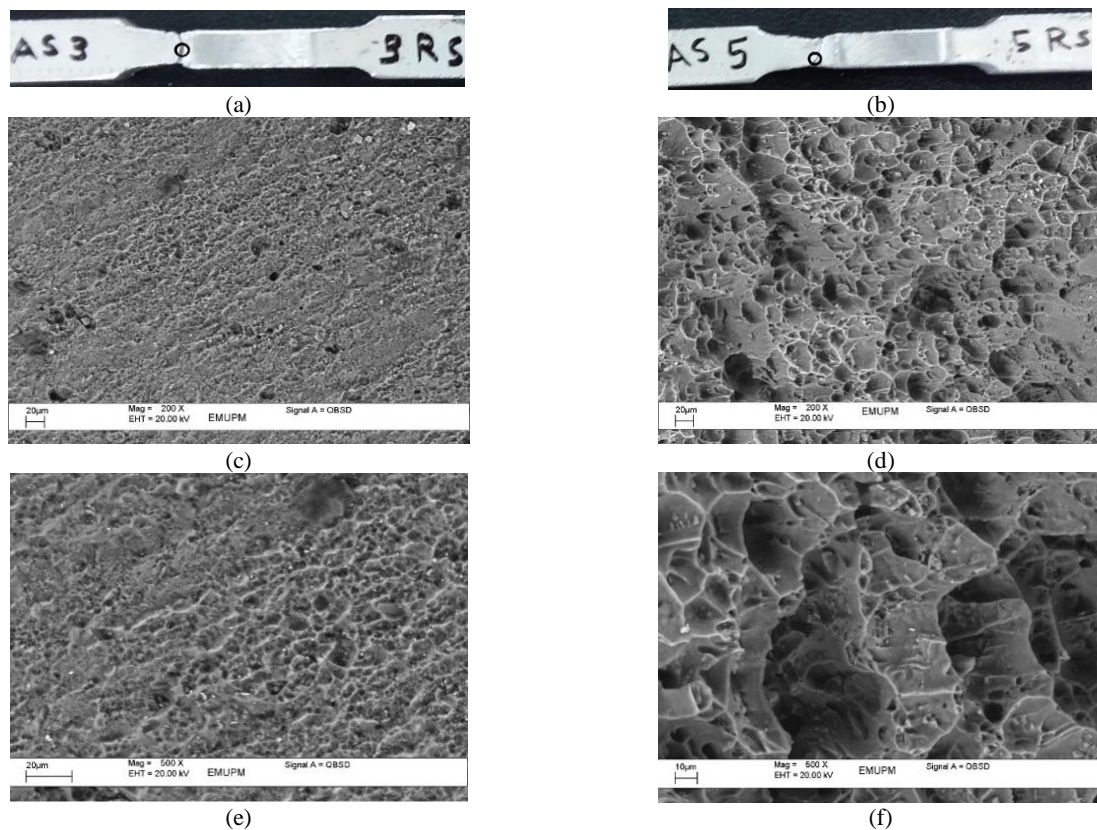
associated with the joints' tensile behavior and the different UTS between these two circumstances is the most marginal. The fractured surfaces have characteristically a higher quantity of almost equal dimples with different sizes (Figure 10 (c) and 10(d)). The fractured surface of the joints made under condition E3 represents shallower dimples in comparison with condition E5. It is also indicated that the joint E3 has further higher hardness compared to E5 as can be seen in the Figure 8 and Table 4. In such a dimple rupture mode, the fracture is mainly caused by the overload and microvoids direct the failure through coalescence. Nucleation of the microvoids may occur near second phase particles, grain boundaries, inclusions, and dislocation pileups.

Figure 10(b) illustrates higher distorted grain characterization in HAZ and TMAZ zone of transverse section. Moreover, relevant sign of distorted grain size is observed, indicating the deformation of material before fracture. It shows more elongation compare to condition E3 (Figure 10(a)), as summarized in Table 4.

Therefore, the microvoids grow and coalesce, thus forming a continuous fracture surface by increasing the strain during tensile testing. Hence, the shallower dimples are formed in condition E3 probably owing to further severe precipitate coarsening occurring during FSW. Hence, in the HAZ of the joints produced under condition E5, less closely spaced Mg<sub>2</sub>Si phase particles are created. During the fracture process, nucleation sites are effectively provided by the second phase particles such as incoherent Mg<sub>2</sub>Si phase and different Al-Fe-Si intermetallic in AA6061 alloy for microvoids. Nevertheless, it is unrealistic to quantitatively measure the quantity of such second-phase particles because the particles are mostly concealed at the bottom of the dimples and possess a color similar to the nearby Al matrix on fractured surfaces under SEM.

**TABLE 4.** Mechanical properties of the dissimilar FSWed in different cross-section

Condition	Mechanical properties				Joint efficiency (%)	Refs.
	UTS (MPa)	YS (MPa)	E (%)	Min H (HV)		
AA6061-T6	310	275	12	110	-	-
Butt joint	245	177	6	-	79	[25]
Butt joint	257.9	-	1.1	78	83	[32]
E1	261.4	179.2	8.1	73.3	84.3	This study
E2	254.7	178.7	8.6	71.9	82.1	This study
E3	262.7	178.6	7.9	74.6	84.7	This study
E4	254.4	176.7	8.4	69.7	82	This study
E5	254.2	177.1	8.2	72.1	82	This study



**Figure 10.** The tensile fractured surfaces under SEM in different conditions E3 and E5: a, c and e) condition E3 and b, d and f) condition E5

## 5. CONCLUSION

In order to improve mechanical properties of dissimilar FSW of AA6061-T6 and AA7075-T6, a new design in cross section of weld joint is presented. The proposed design in cross-section of joint line is a new method to improve the mechanical properties. This study reveal that the different cross-section in joint line has critical effect on the joint efficiency, which is plays an important role in different industries such as automotive, aerospace, electronics and shipbuilding. Friction stir welded joint under four different new design in cross section named E1, E2, E3, E4 and one conventional cross section, E5 were conducted. The mechanical test comes about uncover that the joints welded in all the conditions display exceptionally great ductile properties with UTS higher than 254 MPa and elongation higher than 7%. The highest UTS value which is occurred in E3 condition (Downward step) is 24.7% higher than required for FSW of AA6061 alloy at T6 condition in the American Welding Society (AWS) standard (186 MPa). In addition E3 condition has the best tensile strength which is 2.77 % more than the E5 condition. The weld joint efficiency of the E3 condition (characterized as the proportion of the quality of the weld joint to that of the base metal) accomplished 84.7% of the base metal.

## 6. REFERENCES

1. Fu, B., Qin, G., Li, F., Meng, X., Zhang, J. and Wu, C., "Friction stir welding process of dissimilar metals of 6061-t6 aluminum alloy to az31b magnesium alloy", *Journal of Materials Processing Technology*, Vol. 218, (2015), 38-47. doi: 10.1016/j.jmatprotec.2014.11.039.
2. Rafiee, A., Nickabadi, S., Nobarian, M., Tagimalek, H. and Khatami, H., "Experimental investigation joining al 5083 and high-density polyethylen by protrusion friction stir spot welding containing nanoparticles using taguchi method", *International Journal of Engineering, Transactions C: Aspects*, Vol. 35, No. 6, (2022), 1144-1153. doi: 10.5829/IJE.2022.35.06C.06.
3. Kasman, Ş. and Yenier, Z., "Analyzing dissimilar friction stir welding of aa5754/aa7075", *The International Journal of Advanced Manufacturing Technology*, Vol. 70, No. 1, (2014), 145-156. doi: 10.1007/s00170-013-5256-7.
4. Tiwan, H., Ilman, M. and Kusmono, K., "Effect of pin geometry and tool rotational speed on microstructure and mechanical properties of friction stir spot welded joints in aa2024-o aluminum alloy", *International Journal of Engineering, Transactions B: Applications*, Vol. 34, No. 8, (2021), 1949-1960. doi: 10.5829/IJE.2021.34.08B.16.
5. Mishra, R.S. and Ma, Z., "Friction stir welding and processing", *Materials science and engineering: R: reports*, Vol. 50, No. 1-2, (2005), 1-78. doi: 10.1016/j.msre.2005.07.001.
6. Khatami, H., Azdast, T., Mojaver, M., Hasanzadeh, R. and Rafiei, A., "Study of friction stir spot welding of aluminum/copper dissimilar sheets using taguchi approach", *International Journal*

- of Engineering, Transactions B: Applications*, Vol. 34, No. 5, (2021), 1329-1135. doi: 10.5829/IJE.2021.34.05B.28.
7. Ethiraj, N., Sivabalan, T., Sivakumar, B., Vignesh Amar, S., Vengadeswaran, N. and Vetrivel, K., "Effect of tool rotational speed on the tensile and microstructural properties of friction stir welded different grades of stainless steel joints", *International Journal of Engineering, Transactions A: Basics*, Vol. 33, No. 1, (2020), 141-147. doi: 10.5829/IJE.2020.33.01A.16.
  8. Gibson, B.T., Lammlein, D., Prater, T., Longhurst, W., Cox, C., Ballun, M., Dharmaraj, K., Cook, G. and Strauss, A., "Friction stir welding: Process, automation, and control", *Journal of Manufacturing Processes*, Vol. 16, No. 1, (2014), 56-73. doi: 10.1016/j.jmapro.2013.04.002.
  9. Singh, R., Rizvi, S.A. and Tewari, S., "Effect of friction stir welding on the tensile properties of aa6063 under different conditions", *International Journal of Engineering, Transactions A: Basics*, Vol. 30, No. 4, (2017), 597-603. doi: 10.5829/idosi.ije.2017.30.04a.19.
  10. Torres, E., Graciano-Urbe, J. and Santos, T., "Control of steel detachment and metal flow on aluminum-steel friction stir welding of thin joints", *International Journal of Engineering, Transactions A: Basics*, Vol. 34, No. 4, (2021), 1024-1034. doi: 10.5829/IJE.2021.34.04A.29.
  11. Salah, A.N., Mehdi, H., Mehmood, A., Hashmi, A.W., Malla, C. and Kumar, R., "Optimization of process parameters of friction stir welded joints of dissimilar aluminum alloys aa3003 and aa6061 by rsm", *Materials Today: Proceedings*, Vol. 56, (2022), 1675-1683. doi: 10.1016/j.matpr.2021.10.288.
  12. Cole, E., Fehrenbacher, A., Duffie, N., Zinn, M., Pfeifferkorn, F. and Ferrier, N., "Weld temperature effects during friction stir welding of dissimilar aluminum alloys 6061-t6 and 7075-t6", *The International Journal of Advanced Manufacturing Technology*, Vol. 71, No. 1, (2014), 643-652. doi: 10.1007/s00170-013-5485-9.
  13. Verbičiči, V., Cojocar, R., Bojilă, L.N., Ciucă, C. and Perianu, I.A., "Considerations on the ultimate tensile strength of butt welds of the en aw 5754 aluminium alloy, made by friction stir welding (FSW)", in *Advanced Materials Research, Trans Tech Publ.* Vol. 1157, (2020), 38-46.
  14. Huang, C., Lu, J., Zhu, M., Xu, Y., Li, B., Zhou, Y. and Huang, J., "Oxidation behaviors of the rotary friction welded joints of ht700 superalloy in saturated water steam at 700° c", *Corrosion Communications*, (2022). doi: 10.1016/j.corcom.2021.11.008.
  15. El-Sayed, M.M., Shash, A., Abd-Rabou, M. and ElSherbiny, M.G., "Welding and processing of metallic materials by using friction stir technique: A review", *Journal of Advanced Joining Processes*, Vol. 3, (2021), 100059. doi: 10.1016/j.jajp.2021.100059.
  16. Azeez, S. and Akinlabi, E., "Effect of processing parameters on microhardness and microstructure of a double-sided dissimilar friction stir welded aa6082-t6 and aa7075-t6 aluminum alloy", *Materials Today: Proceedings*, Vol. 5, No. 9, (2018), 18315-18324. doi: 10.1016/j.matpr.2018.06.170.
  17. Avinash, P., Manikandan, M., Arivazhagan, N., Ramkumar, K.D. and Narayanan, S., "Friction stir welded butt joints of aa2024 t3 and aa7075 t6 aluminum alloys", *Procedia Engineering*, Vol. 75, (2014), 98-102. doi: 10.1016/j.proeng.2013.11.020.
  18. Haribalaji, V., Boopathi, S. and Asif, M.M., "Optimization of friction stir welding process to join dissimilar aa2014 and aa7075 aluminum alloys", *Materials Today: Proceedings*, Vol. 50, No., (2022), 2227-2234. doi: 10.1016/j.matpr.2021.09.499.
  19. Prasanth, R. and Hans Raj, K., "Determination of optimal process parameters of friction stir welding to join dissimilar aluminum alloys using artificial bee colony algorithm", *Transactions of the Indian Institute of Metals*, Vol. 71, No. 2, (2018), 453-462. doi: 10.1007/s12666-017-1176-9.
  20. Guo, J., Chen, H., Sun, C., Bi, G., Sun, Z. and Wei, J., "Friction stir welding of dissimilar materials between aa6061 and aa7075 al alloys effects of process parameters", *Materials & Design (1980-2015)*, Vol. 56, (2014), 185-192. doi: 10.1016/j.matdes.2013.10.082.
  21. Kesharwani, R., Panda, S. and Pal, S., "Multi objective optimization of friction stir welding parameters for joining of two dissimilar thin aluminum sheets", *Procedia Materials Science*, Vol. 6, No., (2014), 178-187. doi: 10.1016/j.mspro.2014.07.022.
  22. Peng, G., Ma, Y., Hu, J., Jiang, W., Huan, Y., Chen, Z. and Zhang, T., "Nanoindentation hardness distribution and strain field and fracture evolution in dissimilar friction stir-welded aa 6061-aa 5a06 aluminum alloy joints", *Advances in Materials Science and Engineering*, Vol. 2018, (2018). doi: 10.1155/2018/4873571.
  23. RajKumar, V., VenkateshKannan, M., Sadeesh, P., Arivazhagan, N. and Ramkumar, K.D., "Studies on effect of tool design and welding parameters on the friction stir welding of dissimilar aluminium alloys aa 5052-aa 6061", *Procedia Engineering*, Vol. 75, No., (2014), 93-97. doi: 10.1016/j.proeng.2013.11.019.
  24. Heidarzadeh, A., Javidani, M., Mofarreh, M., Farzaneh, A. and Chen, X.-G., "Submerged dissimilar friction stir welding of aa6061 and aa7075 aluminum alloys: Microstructure characterization and mechanical property", *Metals*, Vol. 11, No. 10, (2021), 1592. doi: 10.3390/met11101592.
  25. Azeez, S., Akinlabi, E., Kailas, S. and Brandi, S., "Microstructural properties of a dissimilar friction stir welded thick aluminum aa6082-t6 and aa7075-t6 alloy", *Materials Today: Proceedings*, Vol. 5, No. 9, (2018), 18297-18306. doi: 10.1016/j.matpr.2018.06.168.
  26. Venkateswarlu, D., Mahapatra, M., Harsha, S.P. and Mandal, N., "Processing and optimization of dissimilar friction stir welding of aa 2219 and aa 7039 alloys", *Journal of Materials Engineering and Performance*, Vol. 24, No. 12, (2015), 4809-4824. doi: 10.1007/s11665-015-1779-4.
  27. Ahmed, M.M., El-Sayed Seleman, M.M., Zidan, Z.A., Ramadan, R.M., Ataya, S. and Alsaleh, N.A., "Microstructure and mechanical properties of dissimilar friction stir welded aa2024-t4/aa7075-t6 t-butt joints", *Metals*, Vol. 11, No. 1, (2021), 128. doi: 10.3390/met11010128.
  28. Torzewski, J., Łazińska, M., Grzelak, K., Szachogłuchowicz, I. and Mierzyński, J., "Microstructure and mechanical properties of dissimilar friction stir welded joint aa7020/aa5083 with different joining parameters", *Materials*, Vol. 15, No. 5, (2022), 1910. doi: 10.3390/ma15051910.
  29. Koilraj, M., Sundareswaran, V., Vijayan, S. and Rao, S.K., "Friction stir welding of dissimilar aluminum alloys aa2219 to aa5083-optimization of process parameters using taguchi technique", *Materials & Design*, Vol. 42, (2012), 1-7. doi: 10.1016/j.matdes.2012.02.016.
  30. Shojaeefard, M.H., Akbari, M., Khalkhali, A., Asadi, P. and Parivar, A.H., "Optimization of microstructural and mechanical properties of friction stir welding using the cellular automaton and taguchi method", *Materials & Design*, Vol. 64, (2014), 660-666. doi: 10.1016/j.matdes.2014.08.014.
  31. Kumar, K.K., Kumar, A. and Satyanarayana, M., "Effect of friction stir welding parameters on the material flow, mechanical properties and corrosion behavior of dissimilar aa5083-aa6061 joints", *Proceedings of the Institution of Mechanical Engineers, Part C: Journal of Mechanical Engineering Science*, Vol. 236, No. 6, (2022), 2901-2917. doi: 10.1177/09544062211036102.
  32. İpekoğlu, G. and Çam, G., "Effects of initial temper condition and postweld heat treatment on the properties of dissimilar friction-stir-welded joints between aa7075 and aa6061 aluminum alloys", *Metallurgical and Materials Transactions A*, Vol. 45, No. 7, (2014), 3074-3087. doi: 10.1007/s11661-014-2248-7.

---

**Persian Abstract**

---

**چکیده**

اتصالات جوشی در فرآیند جوشکاری اصطکاکی اغتشاشی (FSW) توسط گرمای اصطکاکی بوجود آمده جهت اتصال اجزای فلزی جهت ساخت قطعات مورد استفاده قرار می‌گیرد. به دلیل عدم وجود ذوب فاز اصلی، فرآیند FSW چندین مزیت را نسبت به جوشکاری ذوبی ارائه می‌دهد. آلیاژهای AA6XXX و 7XXX AI دو سری از پرکاربردترین مواد ساختاری در صنایع خودروسازی، حمل و نقل ریلی و هوافضا هستند. هدف از این مطالعه بررسی اثر مقطع جدید در خط اتصال و تجزیه و تحلیل جزئیات برای بهبود بیشتر خواص مکانیکی بوده است. اتصال جوشی اصطکاکی اغتشاشی تحت چهار طرح جدید مختلف در مقاطع به نام های E1، E2، E3، E4 و یک مقطع معمولی E5 انجام شده است. اتصالات ساخته شده با استفاده از این روش منجر به نتایج بهتر از نظر استحکام و کیفیت مفصل می‌شود. اتصالات ساخته شده دارای خواص کششی بسیار خوبی با استحکام کششی نهایی (UTS) بالاتر از ۲۵۴ مگاپاسکال و ازدیاد طول بیشتر از ۷٪ است. بالاترین مقدار UTS که در شرایط E3 (گام رو به پایین) رخ داده است، ۲۴۷٪ بیشتر از مقدار مورد نیاز برای FSW آلیاژ AA6061 در شرایط T6 در استاندارد انجمن جوشکاری آمریکا (AWS) (۱۸۶ مگاپاسکال) می‌باشد.

---